cosmetics

MDPI

Article

Combined Treatment of Nicotinamide Mononucleotide and Hyaluronic Acid Attenuates Reactive Oxygen Species and MAPK Signaling in TNF-α-Induced Human Epidermal Keratinocytes

Yea Jung Choi [1,†], Moonseok Kang [2,†], Doeun Kim [3], Dong-Wook Kim [4], Dayeon Ham [5], Gabsik Yang [1], Sullim Lee [6,*] and Ki Sung Kang [1,*]

[1] College of Korean Medicine, Gachon University, Seongnam 13120, Republic of Korea; domdada22@gachon.ac.kr (Y.J.C.); yanggs@gachon.ac.kr (G.Y.)
[2] Wonjin Plastic Surgery Clinic, Seoul 06735, Republic of Korea; flamekms@gmail.com
[3] Massachusetts College of Pharmacy and Health Sciences, Boston, MA 02115, USA; ehdms0801@gmail.com
[4] College of Pharmacy, Wonkwang University, Iksan 54538, Republic of Korea; pharmengin1@wku.ac.kr
[5] College of Literature, Science, and the Arts, University of Michigan, Ann Arbor, MI 48109, USA; liah@umich.edu
[6] Department of Life Science, College of Bio-Nano Technology, Gachon University, Seongnam 13120, Republic of Korea
* Correspondence: sullimlee@gachon.ac.kr (S.L.); kkang@gachon.ac.kr (K.S.K.)
† These authors contributed equally to this work.

Abstract

The accumulation of oxidative damage and inflammation, induced by internal and external factors, represents a major mechanism underlying the aging of skin. Excessive reactive oxygen species (ROS) trigger mitogen-activated protein kinase (MAPK) pathways, upregulating matrix metalloproteinase (MMP) expression and facilitating extracellular matrix degradation. Although nicotinamide mononucleotide (NMN) and hyaluronic acid (HA) possess antioxidant and dermoprotective properties, their potential combinational effects remain largely obscure. This study evaluated the impact of NMN and HA co-treatment on ROS production, MAPK signaling, MMP-1 secretion, and type I collagen secretion in TNF-α-stimulated human epidermal keratinocytes. ROS levels were assessed via DCFDA assay, while MMP-1 and COL1A1 secretion were quantified using ELISA. Additionally, the regulatory effects on ERK, JNK, and p38 phosphorylation were determined by Western blot. Synergy prediction was analyzed using the SynergyFinder platform via Highest Single Agent and Loewe models. While NMN and HA individually attenuated TNF-α-induced ROS and MMP-1 levels, co-treatment provided superior suppression and exhibited combinational interactions at specific concentrations. These findings suggest that NMN and HA combination treatment effectively modulates oxidative stress and skin-aging-related responses by regulating ROS levels and MAPK signaling pathways.

Keywords: Human Epidermal Keratinocytes; reactive oxygen species; nicotinamide mononucleotide; hyaluronic acid

Check for updates

Academic Editor: Maria Letizia Manca

Received: 19 March 2026
Revised: 24 April 2026
Accepted: 28 April 2026
Published: 6 May 2026

Copyright: © 2026 by the authors. Licensee MDPI, Basel, Switzerland. This article is an open access article distributed under the terms and conditions of the Creative Commons Attribution (CC BY) license.

1. Introduction

As the human body's most extensive organ, the skin functions as a critical defense system against various stressors, which are categorized into internal and environmental (intrinsic and extrinsic) factors [1]. Intrinsic factors include the natural decline of cellular function, hormonal changes, and genetic predisposition, whereas extrinsic factors

encompass ultraviolet (UV) radiation, pollutants, and lifestyle influences [2]. These external stimuli trigger inflammatory responses and oxidative stress, with the persistent accumulation of reactive oxygen species (ROS) playing a central role in accelerating skin aging [3].

UV radiation serves as a potent trigger for the upregulated synthesis of diverse pro-inflammatory cytokines within the cutaneous environment, notably TNF-α, IL (interleukin)-8, and IL-6 [4–6]. Among them, TNF-α is recognized as a key mediator that promotes intracellular ROS generation. The accumulation of ROS acts as a stimulus for MAPK and NF-κB signaling, driving the elevated expression of MMPs. These enzymes act as the chief mediators in the degradation of the extracellular matrix scaffold, targeting structural proteins such as elastin and collagen fibers [7–9]. Consequently, the modulation of ROS generation and its associated downstream cascades triggered by TNF-α serves as a pivotal approach for mitigating the skin aging process.

As bioactive compounds, polydeoxyribonucleotide, NMN, and HA are increasingly recognized for their diverse roles in promoting skin wellness and integrity [10–12]. Previous findings indicate that HA effectively stimulates the synthesis of type I collagen while simultaneously attenuating oxidative stress in dermal fibroblasts subjected to UV-A radiation [13]. Beyond its use as a single agent, recent studies have explored combinational strategies involving HA and other bioactive compounds. For instance, co-treatment with HA and polynucleotide in UV-A-induced human dermal fibroblasts demonstrated enhanced protective effects compared to those of single treatments [13]. Additionally, combined treatment with HA and succinic acid (SA) in senescent human dermal fibroblasts induced mitophagy and exhibited anti-aging-related effects [14]. These findings suggest that HA may achieve enhanced functionality when combined with other bioactive molecules.

NMN-mediated mitigation of cellular senescence in human epidermal keratinocytes is underpinned by the suppressive modulation of ROS and aging-related markers, including SA-β-gal and the p21/p16 pathways, coupled with the augmented expression of the cytoprotective factors SIRT3 and NQO1 [15]. In a UV-B-induced SKH-1 hairless mouse photoaging model, oral administration of NMN reduced epidermal thickening, wrinkle formation, and trans-epidermal water loss, while preserving collagen density.

Regarding the underlying molecular mechanisms, the protective effects observed appear to be driven by the coordinated inhibition of MAPK phosphorylation—specifically involving the ERK, JNK, and p38 pathways. This suppressive action was further characterized by a significant decline in the expression of inflammatory mediators like TNF-α and IL-6, as well as the matrix-degrading enzyme MMP-1. Concurrently, the co-treatment facilitated the recovery of HAS-1 and HAS-2 expression, suggesting a robust regulatory influence on both oxidative equilibrium and the structural integrity of the extracellular matrix [16].

The potential effect of combined NMN and HA remains poorly understood, despite the known roles of NMN in oxidative stress regulation and HA in extracellular matrix stability. To address this gap, we investigated how the interaction between these two molecules influences ROS generation and MAPK signaling pathways within a TNF-α-stimulated human epidermal keratinocyte model. The objective was to clarify whether their combined application offers enhanced protective mechanisms compared to individual treatments. To comprehensively evaluate the combined effects of NMN and HA, NMN (5 μM) and HA (5 and 10 μM) were tested individually, along with selected combination treatments (NMN 5 μM with HA 2.5 or 10 μM) in TNF-α-induced human epidermal keratinocytes, based on preliminary screening and relevant literature.

2. Materials and Methods

2.1. HEK Cell Culture and Growth Environment

Human epidermal keratinocytes (HEKs), purchased from PromoCell (Heidelberg, Germany), were cultivated in an atmosphere of 5% CO_2 at 37 °C under humidified conditions. The growth medium, consisting of 1× DMEM (4.5 g/L glucose), (Thermo Fisher Scientific, Waltham, MA, USA) supplemented with 10% Fetal Reserve bovine serum (FBS) and 1% penicillin (10,000 units/mL)–streptomycin (10,000 µg/mL), was refreshed at 72 h intervals for cell culture.

2.2. Sample Preparation

Hyaluronic acid (Cat No. 935166, acid form, Mean MW 25,000 Da) was purchased from Sigma-Aldrich (St. Louis, MO, USA), and NMN (Cat No. 3501, Sigma-Aldrich) in PBS-T tablets (pH7.4, TaKaRa, Shiga, Japan) for cell culture treatment. The initial stock concentration was maintained at 100 mM. To prepare the working solution, recombinant TNF-α protein (PeproTech, Rocky Hill, NJ, USA) was reconstituted in 1% albumin from bovine serum in sterile distilled water (Roche, Basel, Switzerland). For all stimulation assays, TNF-α was introduced to the culture medium at a prescribed final concentration: 20 ng/mL.

2.3. ROS Inhibition Assay

To evaluate ROS production, HEKs were plated in black 96-well plate (1×10^4 cells/well) and stabilized for 24 h (37 °C, 5% CO_2), followed by a 24 h starvation period in serum-free medium [17]. The cells were subsequently exposed to specified concentrations of HA and NMN, administered either individually or in combination, for a 1 h duration. To trigger oxidative stress, a 15 min stimulation was performed using TNF-α (20 ng/mL) and DCFDA (10 µM) cotreatment; the control received only the DCFDA probe. After washing twice with DPBS, intracellular fluorescence was quantified using a microplate reader equipped with fluorescence filters (λex = 485 nm, λem = 535 nm), (Agilent Technologies, Winooski, VT, USA).

2.4. Quantification of Protein Secretion by ELISA

HEKs were seeded in 48-well cell culture plates (2×10^4 cells/well) and cultured for 24 h. Thereafter, with subsequent 24 h starvation in DMEM serum-free medium, the HEK cells were treated with HA and NMN (either alone or in combination) for 1 h. Following this pre-incubation, 20 ng/mL TNF-α was added to stimulate the cells for 24 h. Post-treatment, the culture media were collected and centrifuged to remove cellular debris. MMP-1 and COL1A1 concentrations were then determined using commercial ELISA kits [18]. Spectrophotometric analysis was performed at a wavelength of 450 nm using a microplate reader, in accordance with the manufacturer's specified instructions (Agilent Technologies, Winooski, VT, USA).

2.5. Synergy Finder Analysis

To evaluate potential interactions between NMN and HA, synergy analysis was performed using the SynergyFinder web-based analysis platform (https://synergyfinder.org/, accessed on 18 February 2026). The inhibitory effects of NMN and HA on ROS generation and MMP-1 secretion were normalized by setting the TNF-α-treated group as representing 0% inhibition. The experimental data were then converted into inhibition percentages and uploaded to the SynergyFinder+ platform for further analysis.

Synergy analysis was conducted based on the Highest Single Agent (HSA) and Loewe additivity models provided by the SynergyFinder+ platform. The HSA model evaluates

whether the effect of a drug combination exceeds the maximal effect observed from individual treatments, whereas the Loewe model assesses drug interactions by comparing observed responses with expected additive effects under the assumption that the two agents share similar mechanisms of action. Synergy scores were calculated for each concentration combination and visualized as heatmaps to evaluate the interaction effects of the combined treatments. This analysis was conducted according to previously reported methods [19,20].

2.6. Western Blot Assay

HEKs (3×10^5 cells/well) were plated in a 6-well plate and allowed to attach for 24 h, followed by overnight starvation in serum-depleted media. After a 1 h pre-incubation with HA, NMN, or their combination, 20 ng/mL TNF-α was added to the culture medium for 15 min. To extract proteins, cells were gathered and lysed in RIPA buffer. The resulting lysates were cleared by centrifugation (13,000 rpm, 30 min, 4 °C), and the bicinchoninic acid (BCA) assay (Thermo Fisher Scientific, Waltham, MA, USA) was utilized to determine protein concentrations.

Equal protein masses were separated using 4–20% gradient SDS-PAGE and then electro-wet transferred onto 0.45 μm pore PVDF membranes (Merck, Darmstadt, Germany). To minimize background interference, non-specific binding was inhibited by treating the membranes with 5% non-fat dry milk in TBS-T for a duration of 1 h. This was followed by an overnight incubation under constant refrigeration (4 °C) for an overnight period in 1% albumin from bovine serum solution targeting GAPDH and both the phosphorylated and total forms of MAPKs (specifically p38, JNK, and ERK). After a subsequent washing step, secondary antibodies were applied for 2 h at ambient temperature. Visualization of protein bands was achieved using the Femto substrate, with images recorded on a Western Imaging System (Bio-Rad, Hercules, CA, USA). ImageJ software 1.52a (NIH, Bethesda, MD, USA) was employed for densitometric analysis, with phosphorylation levels normalized to total protein forms and GAPDH as the internal control [21].

2.7. Statistical Analyses

Experimental data are presented as mean ± standard error of the mean (SEM), with the exact sample size (n) specified in each figure caption. We assessed statistical variance among groups using one-way ANOVA. To identify inter-group differences, Tukey's post-analysis was conducted for pairwise comparisons. All computational analyses and graphical representations were generated via GraphPad Prism software (version 8.0; GraphPad Software, San Diego, CA, USA). Differences with $p < 0.05$ were regarded as being statistically significant.

3. Results

3.1. Effect of NMN and HA on Intracellular ROS Generation in TNF-α-Induced HEKs

First, after conducting cytotoxicity assays (Figure S1), the inhibitory effects of NMN and HA on TNF-α-induced ROS generation were evaluated in HEKs.

In Figure 1A, While TNF-α exposure triggered intracellular ROS, adding HA successfully mitigated this effect. Specifically, HA brings ROS levels down to between 1.20 ± 0.07 to 1.29 ± 0.04-fold of the control.

In Figure 1B, We observed a comparable decline in the NMN-treated groups (1.14 ± 0.01 to 1.23 ± 0.06-fold across the tested concentrations).

Interestingly, combined treatment with NMN and HA resulted in a further decrease in ROS levels compared to TNF-α treatment alone. Notably, the lowest ROS levels were observed at higher concentrations, reaching 1.10 ± 0.04-fold under the highest tested condition in Figure 1C.

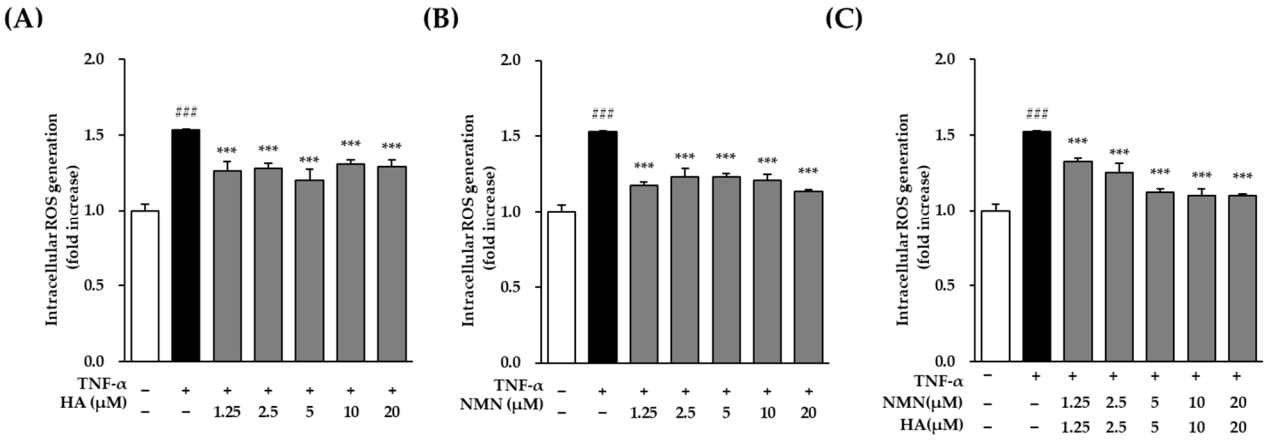


Figure 1. Hyaluronic acid (HA) and nicotinamide mononucleotide (NMN) mitigate the elevation of intracellular ROS triggered by TNF-α exposure. Human epidermal keratinocytes (HEKs) (1×10^4 cells/well) were seeded in black 96-well plates and starved in DMEM serum-free medium for 24 h. Then, after a 1 h pre-incubation with (**A**) HA treatment alone; (**B**) NMN treatment alone; (**C**) combined treatment with HA and NMN, cells were treated with TNF-α (20 ng/mL) and DCFDA (10 μM) cotreatment for 15 min to trigger ROS generation. Fluorescence intensity was then measured at 485/535 nm, with the control group receiving only DCFDA. The data are shown as means ± SEM of triplicate wells (n = 3). For all statistical evaluations, a threshold of $p < 0.001$ was established for significance; specifically, ### denotes a substantial difference relative to the untreated control, while symbols *** represent significant changes compared to the TNF-α-treated group at $p < 0.001$, respectively. White, black, and gray bars represent the control, TNF-α–treated, and compound-treated groups, respectively.

3.2. Potential Combinatorial Interaction of NMN and HA on Intracellular ROS Generation in TNF-α-Induced HEKs

Based on the ROS experimental results, the inhibitory activity was converted into percentage values (Table 1), with the TNF-α-treated group set as the 0% inhibition baseline.

Table 1. Intracellular ROS levels were converted to inhibition rates (%) relative to the TNF-α-induced group. The TNF-α-induced group was defined as 0% inhibition, and the inhibitory effects of individual and combined treatments of HA and NMN were calculated accordingly across the indicated concentration ranges.

Hyaluronic Acid (μM)	Nicotinamide Mononucleotide (μM)	Inhibition Rate (%)
1.25	0	50.41
2.5	0	48.06
5	0	62.13
10	0	41.86
20	0	45.14
0	1.25	67.44
0	2.5	56.33
0	5	56.22
0	10	61.03
0	20	74.08
1.25	1.25	37.66
2.5	2.5	51.74
5	5	76.29
10	10	80.63
20	20	81.30

Combinatorial effects were subsequently analyzed using a HSA model based on the calculated ROS inhibition rates (Figure 2). The analysis indicated that the combination of 2.5 μM HA and 5 μM NMN yielded the highest predicted synergy score (21.81). These findings suggest that NMN and HA may show a combinatorial interaction at specific concentration combinations in TNF-α-induced elevation of intracellular ROS levels.

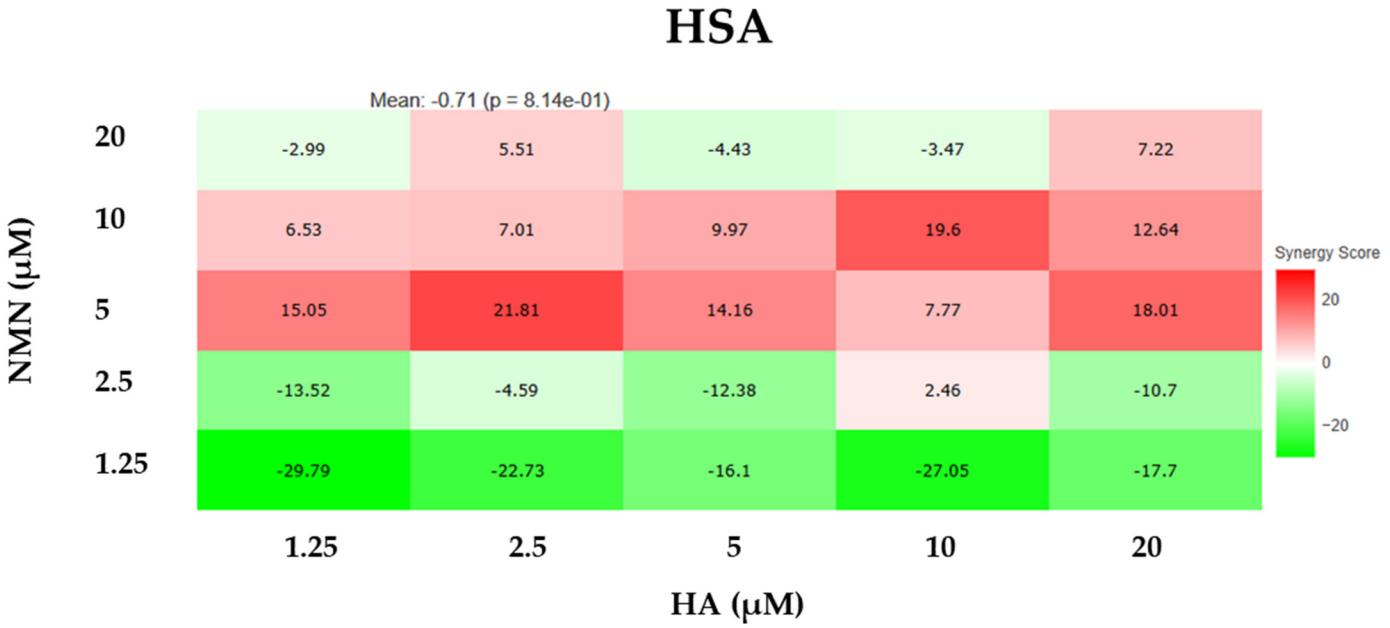


Figure 2. Combinatorial effects of HA and NMN on TNF-α-induced ROS generation in HEKs. Synergy heat maps for the combination of HA and NMN. Synergy scores were calculated using Highest Single Agent (HSA) models based on calculated inhibition rates. The color gradient represents the degree of synergy (red) or antagonism (green) across the tested concentration combinations.

3.3. Effect of NMN and HA on MMP-1, and COL1A1 Secretion in TNF-α-Induced HEKs

Subsequently, the effects of NMN and HA on MMP-1 and COL1A1 protein secretion were evaluated in TNF-α-induced HEKs.

In Figure 3A, NMN treatment alone attenuated TNF-α-induced MMP-1 secretion, with levels ranging from 2.62 ± 0.08-fold (1.25 μM) to 4.91 ± 0.05-fold (20 μM). While HA treatment also led to a reduction in MMP-1, the effect was less pronounced than that of NMN, with values spanning 7.36 ± 0.23 to 8.30 ± 0.05-fold. The combined application of NMN and HA resulted in a further decrease in MMP-1 secretion, maintaining levels between 3.93 ± 0.02 and 6.24 ± 0.58-fold across the tested concentrations.

In Figure 3B, in terms of COL1A1 secretion, NMN only did not produce significant alterations. In contrast, HA treatment increased COL1A1 levels at higher concentrations (0.42 ± 0.05 and 0.45 ± 0.03-fold at 10 and 20 μM, respectively). A similar upward trend was observed under co-treatment conditions, reaching 0.28 ± 0.02-fold at 20 μM.

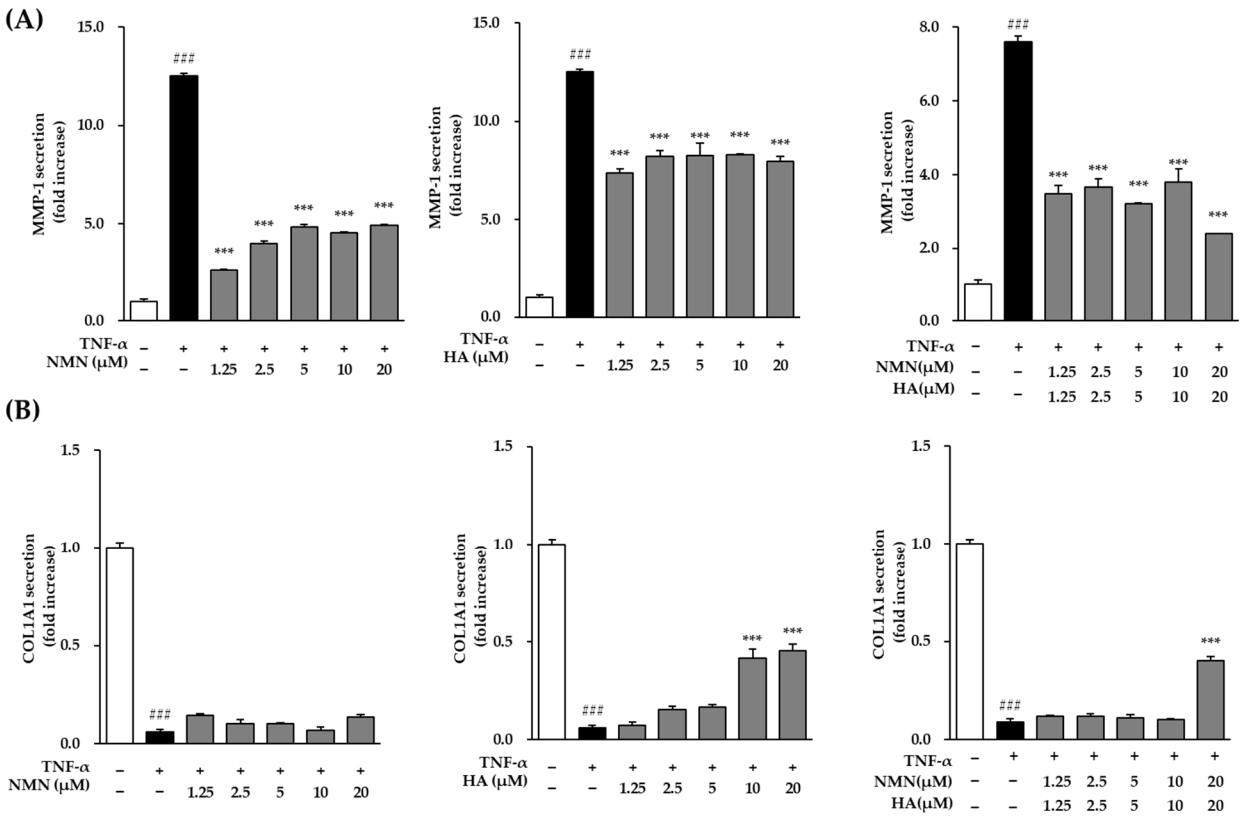


Figure 3. HA and NMN regulate the Secretion of MMP-1 and COL1A1 within HEKs stimulated by TNF-α. Following 1 h of exposure to HA and NMN (individually or combined), HEKs were stimulated with 20 ng/mL TNF-α for 24 h. Subsequently, ELISA was utilized to quantify (**A**) MMP-1 and (**B**) COL1A1 levels in the culture media. Statistical data are indicated as mean ± SEM from duplicate wells (n = 2). For all analyses, $p < 0.001$ was set as the significance threshold, with ### denoting differences relative to the untreated control and *** denoting changes relative to the group treated with TNF-α only. White, black, and gray bars represent the control, TNF-α–treated, and compound-treated groups, respectively.

3.4. Potential Combinatorial Interaction of NMN and HA on MMP-1 Secretion in TNF-α-Induced HEKs

To further assess the combined effects on MMP-1 secretion, the inhibitory responses were converted into percentage values using the TNF-α-induced group as a 0% inhibition reference (Table 2).

Synergy evaluation was subsequently conducted using the Loewe model based on the calculated MMP-1 inhibition rates (Figure 4). The combination of 10 μM HA and 5 μM NMN demonstrated the highest predicted synergy score (27.4). These results suggest potential interactions between NMN and HA at specific concentration combinations in TNF-α-induced MMP-1 secretion.

Table 2. MMP-1 secretion levels expressed as inhibition rates (%) relative to the TNF-α-induced group. The TNF-α-induced group was set as 0% inhibition, and the inhibitory effects of HA and NMN, either alone or in combination, were calculated across the indicated concentration ranges.

Hyaluronic Acid (μM)	Nicotinamide Mononucleotide (μM)	Inhibition Rate (%)
1.25	0	44.74
2.5	0	37.28
5	0	36.84
10	0	36.62
20	0	39.69
0	1.25	85.96
0	2.5	74.12
0	5	66.89
0	10	69.52
0	20	66.01
1.25	1.25	59.14
2.5	2.5	56.6
5	5	62.73
10	10	54.49
20	20	74.55

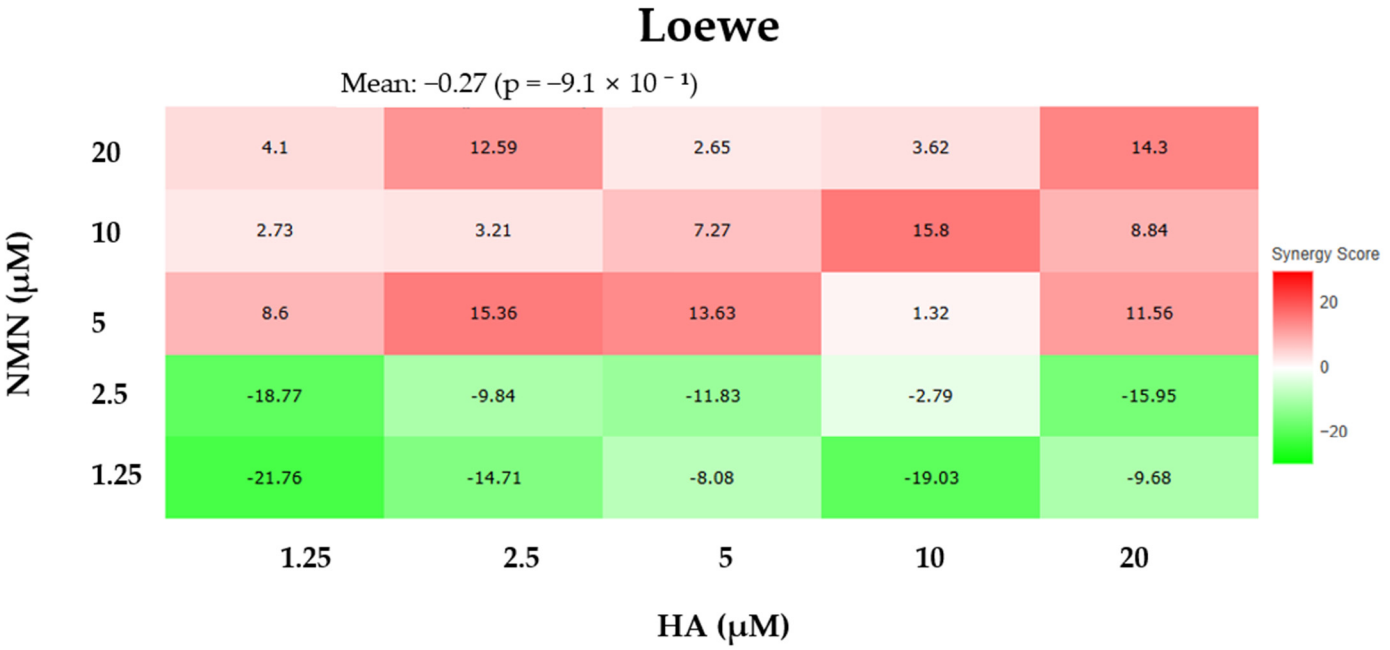


Figure 4. Combinatorial effects of HA and NMN on TNF-α-induced MMP-1 secretion in HEKs. Synergy heat maps illustrating the combinatorial effects of HA and NMN administration. Synergy scores were determined using the Loewe additivity model based on calculated inhibition rates. The color scale indicates the degree of synergy (red) or antagonism (green) across the tested concentration combinations.

3.5. Combinatorial Effect of NMN and HA on Intracellular ROS Generation, MMP-1 and COL1A1 Secretion in TNF-α-Induced HEKs

Based on the synergy analysis results, two combination treatments (NMN 5 μM + HA 2.5 μM and NMN 5 μM + HA 10 μM) were further evaluated in TNF-α-induced HEKs to determine their effect on ROS production along with the release of MMP-1 and COL1A1.

In Figure 5A, Co-treatment with NMN and HA effectively reduced ROS levels compared to the TNF-α-induced group. ROS accumulation decreased from 1.99 ± 0.03-fold to

1.53 ± 0.03-fold with 5 μM NMN and 2.5 μM HA, and further declined to 1.38 ± 0.02-fold with 10 μM HA.

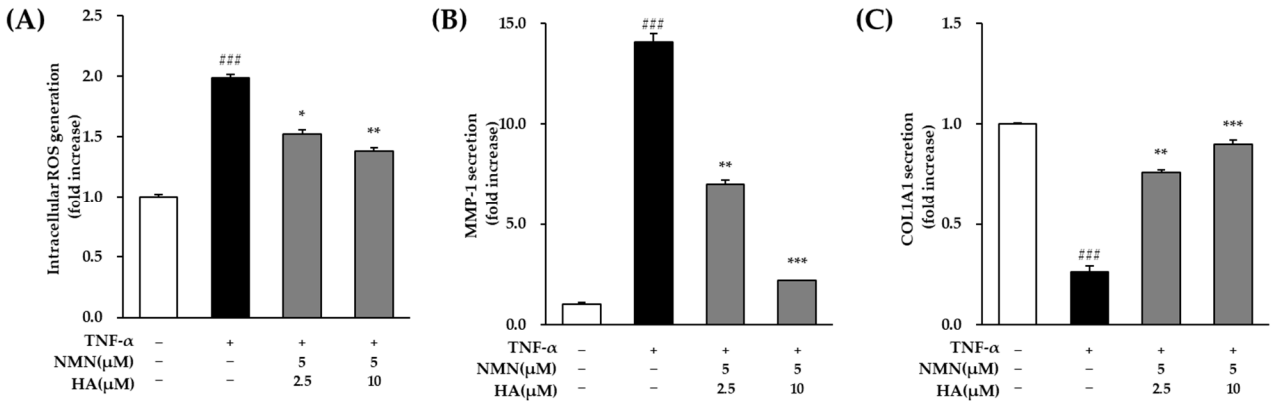


Figure 5. Combinational Inhibition of TNF-α-Induced ROS and Extracellular Matrix (ECM) Degradation by HA and NMN in HEKs. HEKs were pretreated with HA, NMN, or their combination (HA + NMN) for 1 h prior to TNF-α (20 ng/mL) stimulation. (**A**) For intracellular ROS analysis, DCFDA (10 μM) was added to the cells, and fluorescence was determined with a microplate reader equipped with fluorescence filters. Values of ROS assay results are expressed as the mean ± standard error (SEM) of triplicate wells (n = 3). (**B**,**C**) For extracellular matrix-related protein analysis, cells were induced with TNF-α for 24 h, and the protein secretion levels were measured by ELISA. Results are expressed as means ± SEM of duplicate wells (n = 2). For all statistical evaluations, $p < 0.001$ (###) indicated a significant difference from the untreated control. Comparisons against the TNF-α-treated group were marked by asterisks representing p-values of less than 0.05 (*), 0.01 (**), and 0.001 (***). White, black, and gray bars represent the control, TNF-α–treated, and compound-treated groups, respectively.

In Figure 5B, a similar pattern was observed for MMP-1 secretion, which dropped from 14.08 ± 0.39-fold (TNF-α alone) to 6.99 ± 0.21 and 2.17 ± 0.02-fold under the respective co-treatment conditions.

In contrast, in Figure 5C, COL1A1 secretion showed an increasing trend following the combined treatment. Specifically, levels rose from 0.26 ± 0.03-fold to 0.76 ± 0.01-fold and 0.90 ± 0.02-fold at the same concentrations of NMN and HA (2.5 and 10 μM HA with 5 μM NMN).

3.6. Combinatorial Effect of NMN and HA on MAPK Expression in TNF-α-Induced HEKs

Next, the regulatory impact of combined NMN and HA on MAPK phosphorylation was further examined in TNF-α-induced HEKs via immunoblotting in Figure 6A.

In Figure 6B, TNF-α stimulation significantly induced ERK phosphorylation, reaching 13.08 ± 0.1-fold relative to the control. This activation was attenuated by 10 μM HA (7.61 ± 0.2-fold), and a comparable reduction was noted under the co-treatment of 5 μM NMN and 2.5 μM HA (8.59 ± 0.46-fold).

A similar trend was evident in JNK phosphorylation; the TNF-α-induced increase (10.25 ± 0.17-fold) was suppressed to 5.32 ± 0.3-fold by HA treatment, with a further decline to 4.3 ± 0.25-fold observed under co-treatment conditions.

Regarding the p38 pathway, TNF-α elevated phosphorylation to 7.17 ± 0.04-fold. While 5 μM NMN alone exerted a modest inhibitory effect (6.21 ± 0.05-fold), 10 μM HA led to a more distinct decrease (5.53 ± 0.14-fold). Notably, the most substantial suppression occurred with the combination of 5 μM NMN and 10 μM HA, which brought p-p38 levels down to 3.44 ± 0.08-fold.

Overall, ERK and JNK phosphorylation were suppressed under HA (10 μM) and NMN (5 μM) + HA (2.5 μM) treatment conditions, whereas p38 inhibition was more pronounced in the NMN (5 μM) + HA (10 μM) group.

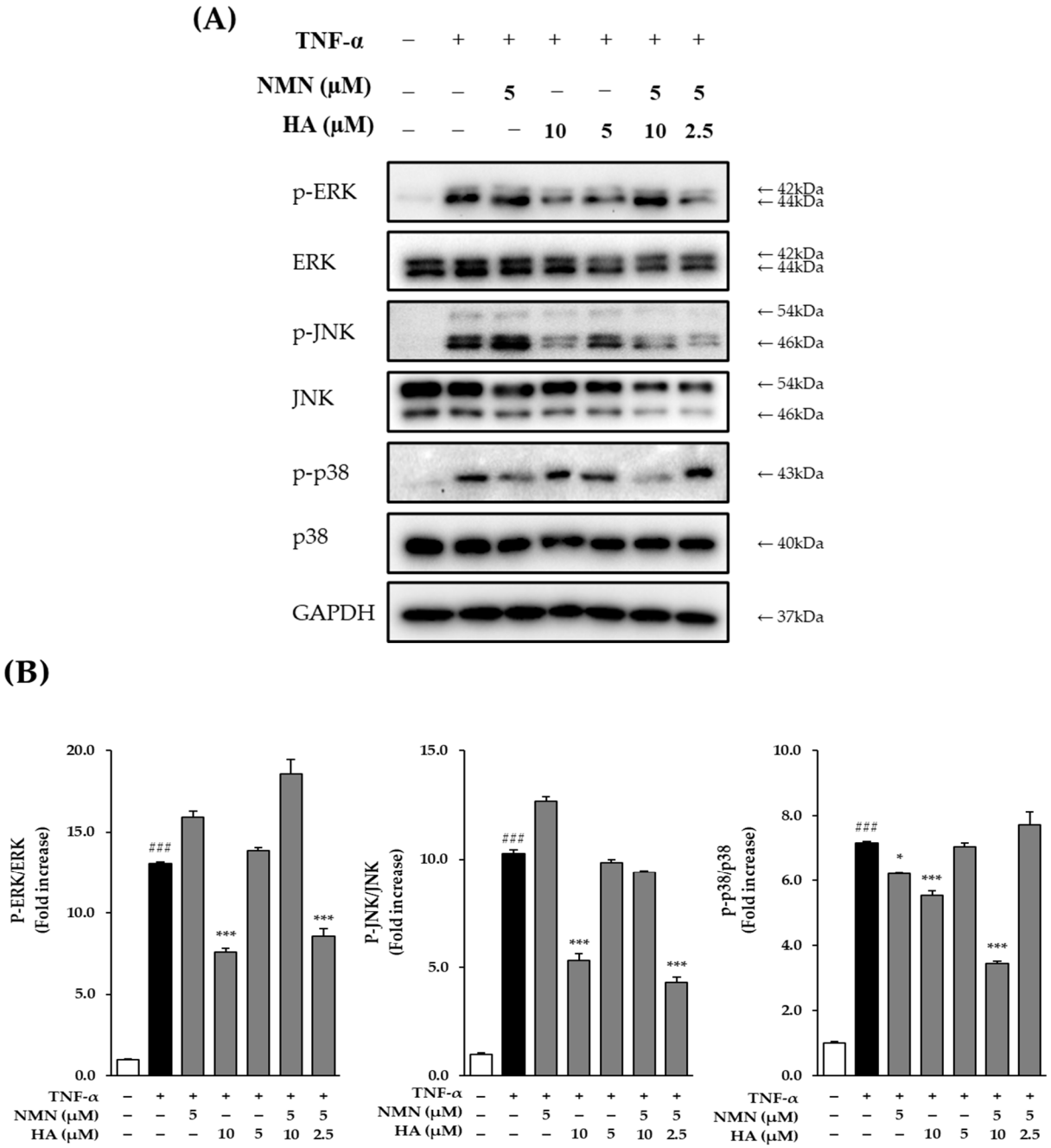


Figure 6. Combinatorial effects of HA and nicotinamide mononucleotide on TNF-α-induced phosphorylation of MAPKs in HEKs. (**A**) To examine MAPK activation, HEKs were primed with specific concentrations of HA and NMN (alone or co-treatment) for 60 min before a TNF-α exposure (20 ng/mL) for 15 min duration. Levels of phosphorylated JNK, ERK, and p38 were determined via immunoblotting; total MAPK species and GAPDH were utilized to ensure equal protein loading. (**B**) Relative phosphorylation levels for each kinase are depicted as fold changes normalized to the untreated baseline. Each value represents the mean ± SEM from three independent experimental replicates (n = 3). Statistical thresholds are defined as: ### $p < 0.001$ versus the control; significant differences from the TNF-α-induced group are indicated by p-values of less than 0.05 (*) and 0.001 (***). White, black, and gray bars represent the control, TNF-α–treated, and compound-treated groups, respectively.

4. Discussion

The current study aimed to evaluate the effects of a combined treatment of NMN and HA on ROS generation, MAPK signaling activation, MMP-1 secretion, and collagen type I production in TNF-α-induced human epidermal keratinocytes. The pathogenesis of various skin pathologies, ranging from atopic dermatitis to skin cancer and psoriasis, is intimately linked to oxidative stress, which is recognized for its capacity to hasten the aging process of the skin [22]. Therefore, ROS plays an important role in maintaining skin health and physiological balance.

As shown in Figure 1, the combined treatment with NMN and HA at a 1:1 ratio more effectively suppressed ROS generation at low concentrations (1.25 and 2.5 μM) compared with each treatment alone. Previous studies have reported that NMN and HA exhibit antioxidant properties by reducing ROS production in skin cells [13,15]. Our findings suggest that their antioxidant activities may act in a complementary manner under combined treatment, thereby contributing to the regulation of TNF-α-induced oxidative stress.

In Figure 3, the effect of the combined treatment of NMN and HA on MMP-1 secretion was evaluated. The results showed that the combined treatment significantly inhibited MMP-1 secretion in the 20 μM condition compared with those of single treatments. Supporting these findings, the suppression of MMP-1 by NMN and HA has been observed in both human epidermal keratinocytes and skin equivalent models [23,24]. Our findings indicate that the effects of NMN and HA on skin-aging-related responses may act in a complementary manner under selected concentration conditions to regulate TNF-α-induced MMP-1 secretion.

Based on the results presented in Figures 1 and 3, the interaction between NMN and HA was further evaluated, as presented in Figures 2 and 4, by applying the two compounds at a 1:1 ratio and analyzing their effects on the secretory profiles of MMP-1 and COL1A1. The data indicated that the combination of HA (10 μM) and NMN (5 μM) significantly reduced MMP-1 secretion compared with those in the single-treatment groups. In contrast, collagen type I secretion did not demonstrate a consistent increase across all combination conditions. However, significant increases were observed in the HA 10 μM + NMN 5 μM and HA 2.5 μM + NMN 5 μM groups. These results demonstrate that the co-treatment of the two compounds is not uniformly synergistic across all concentrations, but instead represents a concentration-dependent interaction under specific conditions. Additionally, it has been shown that HA promotes COL1A1 expression, whereas NMN stimulates the secretion of type I collagen within human dermal fibroblasts [13,25]. Therefore, the combined effect of NMN and HA may be better interpreted as a complementary regulatory interaction depending on concentration rather than a consistent additive effect.

ROS-induced activation of MAPK signaling in skin cells promotes collagen degradation through the upregulation of MMP-1, thereby contributing to wrinkle formation [26]. Moreover, MAPK signaling pathways trigger the activation of transcription factors including AP-1 and NF-κB, which in turn induces the production of pro-inflammatory cytokines such as IL-1β, IL-8, and IL-6 [27,28]. Therefore, regulation of MAPK signaling is considered an important mechanism in controlling skin aging and inflammatory responses.

The mechanistic effects of NMN and HA on MAPK signaling are presented in Figure 6. Phosphorylation levels of ERK and JNK were notably attenuated in the HA 10 μM and NMN 5 μM + HA 2.5 μM groups, while p38 phosphorylation was significantly inhibited in the NMN 5 μM, HA 10 μM, and NMN 5 μM + HA 10 μM groups. Previous studies have reported that NMN suppresses the phosphorylation of ERK, JNK, and p38 MAPKs in UV-induced mouse models of skin aging [16]. In contrast, studies investigating the effects of HA on MAPK signaling in skin cells remain limited. Although MAPK inhibition in this study did not exhibit a clear concentration-dependent pattern, the combined treatment of

NMN and HA modulated MAPK phosphorylation under selected treatment conditions, although the effects were not uniform across all pathways and concentrations.

Collectively, combined treatment with NMN and HA attenuated oxidative stress in TNF-α-induced HEKs and reduced MMP-1 secretion under specific concentration conditions. In addition, phosphorylation of MAPK subfamilies, including ERK, JNK, and p38, was modulated under certain treatment conditions. These results demonstrate that the combined treatment of NMN and HA may help attenuate skin-aging-related responses, partially mediated by the regulation of ROS levels and MAPK-mediated signaling pathways under specific experimental conditions.

To further interpret these findings, potential underlying mechanisms may be considered. NMN has been reported to enhance intracellular NAD^+ levels and regulate mitochondrial and redox-related pathways, leading to a reduction in intracellular ROS levels. In addition, excessive ROS generation is known to activate MAPK signaling pathways, which subsequently induce the secretion of MMP-1 in skin cells. Accordingly, the suppression of MAPK signaling by NMN observed here is likely linked to the regulation of ROS via NAD^+-mediated metabolic processes [15,29].

In addition, previous studies have reported that HA can modulate inflammatory responses through TLR4-mediated signaling pathways in keratinocytes. Furthermore, TLR4 activation has been shown to regulate MAPK signaling, including ERK pathways, leading to the expression of pro-inflammatory cytokines and MMPs in skin-related cells. Collectively, our data indicate that the HA-induced attenuation of MAPK signaling reported here potentially involves the regulation of TLR4-mediated pathways [30,31].

Taken together, these findings indicate that the combined effects of NMN and HA observed in this study may be partly explained by their complementary mechanisms, involving NMN-mediated intracellular redox regulation and HA-mediated receptor-dependent signaling pathways, both of which converge on the modulation of MAPK signaling.

However, this study has some limitations. First, the mechanistic investigation was conducted only in HEKs, which are primarily distributed in the epidermal layer of the skin. Therefore, additional studies involving human dermal fibroblasts, which are predominantly located in the dermal layer, are required [32]. Furthermore, validation using 3D co-culture models of keratinocytes and dermal fibroblasts, as well as in vivo studies using hairless mouse models, would provide a more comprehensive evaluation of the skin-protective effects of combined treatment of NMN and HA [33,34]. For example, in vivo validation using a UVB-induced photoaging model in SKH-1 hairless mice could be conducted by evaluating MAPK signaling pathways and AP-1 activation (e.g., p-c-Jun and p-c-Fos) in skin tissues following topical treatment. Furthermore, histological evaluation via Masson's trichrome and hematoxylin and eosin (H&E) staining facilitates the characterization of structural alterations across the dermis and epidermis [35,36].

5. Conclusions

In conclusion, we evaluated the effects of combined NMN and HA treatment on oxidative stress and skin-aging-related signaling pathways in TNF-α-induced human epidermal keratinocytes. The results showed that co-treatment suppressed ROS generation and reduced MMP-1 secretion under specific concentration conditions, while modulating MAPK signaling pathways in a pathway-specific manner depending on the treatment conditions. These findings suggest that NMN and HA may exert complementary effects under certain conditions, rather than consistent synergistic effects. However, further studies using dermal fibroblasts and in vivo animal models are warranted to validate their biological significance to skin-aging-related responses.

Supplementary Materials: The following supporting information can be downloaded at: https://www.mdpi.com/article/10.3390/cosmetics13030116/s1, Figure S1: Effects of NMN and HA on cell viability in human epidermal keratinocytes (HEKs).

Author Contributions: Methodology, M.K., D.K., D.H. and D.-W.K., validation, G.Y., Writing—original draft preparation, Y.J.C., D.H. and M.K.; formal analysis, Y.J.C., D.K., D.-W.K. and G.Y. supervision; S.L. and K.S.K.; project administration, S.L. and K.S.K. All authors have read and agreed to the published version of the manuscript.

Funding: This research was supported by the Bio & Medical Technology Development Program of the National Research Foundation (NRF) funded by the Korean government (MSIT) (No. RS-2025-02263193) and (No. RS-2024-00463053).

Institutional Review Board Statement: Not applicable.

Informed Consent Statement: Not applicable.

Data Availability Statement: All data generated or analyzed during this study are included in this published article.

Acknowledgments: During the preparation of this manuscript, the authors used ChatGPT (OpenAI, GPT-5.3) for language editing purposes. The authors have reviewed and edited the output and take full responsibility for the content of this publication.

Conflicts of Interest: M.K. is employed by Wonjin Plastic Surgery Clinic, Seoul, Republic of Korea. The company had no role in the design of the study; in the collection, analyses, or interpretation of data; in the writing of the manuscript; or in the decision to publish the results.

Abbreviations

The following abbreviations are used in this manuscript:

AP-1	Activator Protein-1
COL1A1	Collagen Type I Alpha 1 Chain
ELISA	Enzyme-Linked Immunosorbent Assay
ERK	Extracellular Signal-Regulated Kinase
HA	Hyaluronic Acid
HAS-1	Hyaluronan Synthase 1
HAS-2	Hyaluronan Synthase 2
HDF	Human Dermal Fibroblasts
HEK	Human Epidermal Keratinocyte
IL-1β	Interleukin-1 beta
IL-6	Interleukin-6
IL-8	Interleukin-8
JNK	c-Jun N-terminal Kinase
MAPK	Mitogen-Activated Protein Kinase
MMP-1	Matrix Metalloproteinase-1
NF-κB	Nuclear Factor kappa-light-chain-enhancer of activated B cells
NMN	Nicotinamide Mononucleotide
NQO1	NAD(P)H Quinone Dehydrogenase 1
p16	Cyclin-Dependent Kinase Inhibitor 2A
p21	Cyclin-Dependent Kinase Inhibitor 1A
p38	p38 Mitogen-Activated Protein Kinase
ROS	Reactive Oxygen Species
SIRT3	Sirtuin 3
TNF-α	Tumor Necrosis Factor-alpha
UV	Ultraviolet Radiation

References

1. Sullivan, J.V.; Myers, S. Skin structure and function, wound healing and scarring. In *Plastic Surgery-Principles and Practice*; Elsevier: Amsterdam, The Netherlands, 2022; pp. 1–14. [CrossRef]
2. Hussein, R.S.; Bin Dayel, S.; Abahussein, O.; El-Sherbiny, A.A. Influences on skin and intrinsic aging: Biological, environmental, and therapeutic insights. *J. Cosmet. Dermatol.* **2025**, *24*, e16688. [CrossRef]
3. Krutmann, J.; Schikowski, T.; Morita, A.; Berneburg, M. Environmentally-induced (extrinsic) skin aging: Exposomal factors and underlying mechanisms. *J. Investig. Dermatol.* **2021**, *141*, 1096–1103. [CrossRef] [PubMed]
4. Garimano, N.; Aguayo Frías, T.; González Maglio, D.H. Beyond ultraviolet radiation: Immune system modulation through skin exposure to visible light and infrared radiation. *Photochem. Photobiol.* **2025**, *101*, 846–857. [CrossRef] [PubMed]
5. Lim, S.H.; Seo, H.-S.; Kang, H.; Hong, S.-P. Red ginseng-derived components attenuate UVB-induced keratinocyte senescence via senomorphic mechanisms. *J. Ginseng Res.* **2026**, *50*, 101018. [CrossRef]
6. Jang, H.-Y.; Kim, G.-B.; Kim, J.-M.; Kang, S.Y.; Youn, H.-J.; Park, J.; Ro, S.Y.; Chung, E.-Y.; Park, K.-H.; Kim, J.-S. Fisetin inhibits UVA-induced expression of MMP-1 and MMP-3 through the NOX/ROS/MAPK pathway in human dermal fibroblasts and human epidermal keratinocytes. *Int. J. Mol. Sci.* **2023**, *24*, 17358. [CrossRef]
7. Ahn, S.-Y.; Jeong, S.Y.; Lee, B.S.; Joh, Y.S.; Hamishehkar, H.; Lee, S.; Kim, K.H. Anti-skin aging potential of methoxyflavones from Kaempferia parviflora against TNF-α-induced oxidative stress and photoaging in normal human dermal fibroblasts. *Foods* **2025**, *14*, 4012. [CrossRef]
8. Van Doren, S.R. Matrix metalloproteinase interactions with collagen and elastin. *Matrix Biol.* **2015**, *44–46*, 224–231. [CrossRef]
9. Keet, L.; Magcwebeba, T.; Abel, S.; Louw, A.; Gelderblom, W.; Lilly, M. Modulation of UVB-induced oxidative stress and inflammation in skin keratinocytes (HaCaT) utilising unfermented rooibos and honeybush aqueous extracts. *J. Photochem. Photobiol.* **2024**, *22*, 100242. [CrossRef]
10. Park, S.; Baek, S.; Shin, H.-J.; Kim, J.-S.; Gwon, H.-I.; Bae, S.; An, S. Polydeoxyribonucleotides as emerging therapeutics for skin diseases: Clinical applications, pharmacological effects, molecular mechanisms, and potential modes of action. *Appl. Sci.* **2025**, *15*, 10437. [CrossRef]
11. Soma, M.; Lalam, S.K. The role of nicotinamide mononucleotide (NMN) in anti-aging, longevity, and its potential for treating chronic conditions. *Mol. Biol. Rep.* **2022**, *49*, 9737–9748. [CrossRef]
12. Al-Halaseh, L.K.; Al-Jawabri, N.A.; Tarawneh, S.K.; Al-Qdah, W.K.; Abu-Hajleh, M.N.; Al-Samydai, A.M.; Ahmed, M.A. A review of the cosmetic use and potentially therapeutic importance of hyaluronic acid. *J. Appl. Pharm. Sci.* **2022**, *12*, 034–041. [CrossRef]
13. Tran, T.T.T.; Heo, S.C.; Lee, J.H.; Kim, H.-W. Synergistic protective and regenerative effects of hyaluronic acid and polynucleotides against UVA-induced oxidative stress in dermal fibroblasts. *Sci. Rep.* **2026**, *16*, 6703. [CrossRef]
14. Martinez-Gutierrez, A.; Cami, H.; Noya, T.; Gómez-Escalante, S.; Miró Llosas, A.; González, M.C. Hyaluronic and succinic acid: New biostimulating combination to counteract dermal and subcutaneous aging. *Int. J. Mol. Sci.* **2025**, *26*, 7548. [CrossRef]
15. Choi, Y.J.; Kang, M.; Jin, M.H.; Kim, J.; Lee, W.K.; Roh, S.-S.; Kang, K.S.; Hwang, G.S.; Park, S.; Lee, S. Fermented porcine placenta and its dipeptides modulate cellular senescence in human keratinocytes. *Curr. Issues Mol. Biol.* **2025**, *47*, 941. [CrossRef] [PubMed]
16. Kim, S.J.; Lee, S.; Choi, Y.J.; Kang, M.; Lee, J.; Hwang, G.S.; Roh, S.-S.; Jin, M.H.; Park, S.; Park, M.; et al. β-Nicotinamide mononucleotide Enhances Skin Barrier Function and Attenuates UV-B-Induced Photoaging in Mice. *Antioxidants* **2025**, *14*, 1424. [CrossRef]
17. Truong, V.-L.; Bae, Y.-J.; Bang, J.-H.; Jeong, W.-S. Combination of red ginseng and velvet antler extracts prevents skin damage by enhancing the antioxidant defense system and inhibiting MAPK/AP-1/NF-κB and caspase signaling pathways in UVB-irradiated HaCaT keratinocytes and SKH-1 hairless mice. *J. Ginseng Res.* **2024**, *48*, 323–332. [CrossRef]
18. Kim, K.M.; Im, A.-R.; Shim, K.-S.; Seo, C.-S.; Lee, Y.; Lee, J.; Yoo, J.S.; Choi, S.; Chae, S. Chikusetsusaponin IVa from *Dolichos lablab* Linne attenuates UVB-induced skin photoaging in mice by suppressing MAPK/AP-1 signaling. *Appl. Biol. Chem.* **2024**, *67*, 79. [CrossRef]
19. Ianevski, A.; He, L.; Aittokallio, T.; Tang, J. SynergyFinder: A web application for analyzing drug combination dose–response matrix data. *Bioinformatics* **2017**, *33*, 2413–2415. [CrossRef]
20. Ianevski, A.; Giri, A.K.; Aittokallio, T. SynergyFinder 2.0: Visual analytics of multi-drug combination synergies. *Nucleic Acids Res.* **2020**, *48*, W488–W493. [CrossRef] [PubMed]
21. Tran, N.K.S.; Nguyen, N.Q.; Lee, S.; Kim, S.H.; Jeong, D.; Seo, E.; Park, J.J.; Cho, J.; Kang, K.S. Anticancer effects of aloe-emodin from Rheum undulatum L. through activation of the p53 pathway in human prostate cancer cells. *Appl. Biol. Chem.* **2024**, *67*, 102. [CrossRef]
22. Nakai, K.; Tsuruta, D. What are reactive oxygen species, free radicals, and oxidative stress in skin diseases? *Int. J. Mol. Sci.* **2021**, *22*, 10799. [CrossRef]
23. Zhang, Y.; Ai, C.; Huang, F.; Zhao, J.-L.; Ling, Y.; Chen, W.; Li, Z.; Wang, Y.; Gao, F.; Li, S.; et al. β-Nicotinamide mononucleotide blocks UVB-induced collagen reduction via regulation of ROS/MAPK/AP-1 and stimulation of mitochondrial proline biosynthesis. *Photochem. Photobiol. Sci.* **2025**, *24*, 293–306. [CrossRef]

24. Chen, F.; Guo, X.; Wu, Y. Skin antiaging effects of a multiple mechanisms hyaluronan complex. *Skin Res. Technol.* **2023**, *29*, e13350. [CrossRef] [PubMed]
25. Betsuno, R.; Yamane, T.; Tsuji, H.; Nakajima, Y.; Imai, M.; Bamba, T.; Uchiyama, S. Permeation of nicotinamide mononucleotide (NMN) in an artificial membrane as a cosmetic skin permeability test model. *J. Cosmet. Dermatol.* **2025**, *24*, e70222. [CrossRef] [PubMed]
26. Yun, J.; Kim, J.-E. Luteolin targets MKK4 to attenuate particulate matter-induced MMP-1 and inflammation in human keratinocytes. *Sci. Rep.* **2025**, *15*, 16848. [CrossRef]
27. Lee, S.; Choi, Y.J.; Lee, S.; Kang, K.S.; Jang, T.S.; Kim, K.H. Protective effects of withagenin A diglucoside from Indian ginseng (Withania somnifera) against human dermal fibroblast damaged by TNF-α stimulation. *Antioxidants* **2022**, *11*, 2248. [CrossRef]
28. Lim, C.-M.; Kim, N.-Y.; Kim, J.; Park, H.-M.; Lee, H.-P.; Hong, J.-T.; Kwon, D.O.; Choi, K.; Yoon, D.-Y. MMPP attenuates the inflammatory response by suppressing ROS and proinflammatory cytokine and chemokine production in TNF-α/IFN-γ-Stimulated human keratinocytes. *J. Microbiol. Biotechnol.* **2025**, *35*, e2508045. [CrossRef] [PubMed]
29. Ahn, S.-Y.; Lee, S.; Kim, D.; Lee, S. Evaluation of the Antiaging Potential of the Dendropanax morbiferus-Derived Compound Dendropanoxide in TNF-α-Stimulated Human Dermal Fibroblasts. *Curr. Issues Mol. Biol.* **2025**, *47*, 188. [CrossRef]
30. Hu, L.; Nomura, S.; Sato, Y.; Takagi, K.; Ishii, T.; Honma, Y.; Watanabe, K.; Mizukami, Y.; Muto, J. Anti-inflammatory effects of differential molecular weight Hyaluronic acids on UVB-induced calprotectin-mediated keratinocyte inflammation. *J. Dermatol. Sci.* **2022**, *107*, 24–31. [CrossRef]
31. Seo, S.-W.; Park, S.-K.; Oh, S.-J.; Shin, O.S. TLR4-mediated activation of the ERK pathway following UVA irradiation contributes to increased cytokine and MMP expression in senescent human dermal fibroblasts. *PLoS ONE* **2018**, *13*, e0202323. [CrossRef]
32. Lee, W.; Debasitis, J.C.; Lee, V.K.; Lee, J.-H.; Fischer, K.; Edminster, K.; Park, J.-K.; Yoo, S.-S. Multi-layered culture of human skin fibroblasts and keratinocytes through three-dimensional freeform fabrication. *Biomaterials* **2009**, *30*, 1587–1595. [CrossRef] [PubMed]
33. Fedeli, V.; Cucina, A.; Dinicola, S.; Fabrizi, G.; Catizone, A.; Gesualdi, L.; Ceccarelli, S.; Harrath, A.H.; Alwasel, S.H.; Ricci, G.; et al. Microgravity modifies the phenotype of fibroblast and promotes remodeling of the fibroblast–keratinocyte interaction in a 3D Co-culture model. *Int. J. Mol. Sci.* **2022**, *23*, 2163. [CrossRef]
34. Budluang, P.; Kim, J.E.; Park, E.S.; Seol, A.; Jang, H.J.; Kang, M.S.; Kim, Y.H.; Choi, J.; Kim, S.; Kim, S.; et al. N-benzyl-N-methyldecane-1-amine derived from garlic ameliorates UVB-induced photoaging in HaCaT cells and SKH-1 hairless mice. *Sci. Rep.* **2025**, *15*, 6979. [CrossRef] [PubMed]
35. Song, H.-A.; Park, M.-J.; Lee, C.-W.; Park, S.; Lee, J.K.; Chung, K.-S.; Lee, K.-T. Anti-Photoaging Effects of a Standardized Hot Water Extract of Petasites japonicus Leaves in Ultraviolet B-Exposed Hairless Mice. *Pharmaceuticals* **2025**, *18*, 1490. [CrossRef] [PubMed]
36. Park, M.-J.; Song, N.-E.; Song, H.-A.; Chung, K.-S.; An, H.-J.; Hong, H.-D.; Choi, S.Y.; Rhee, Y.K.; Lee, K.-T. Standardized hot water extract from the aerial parts of Cirsium setidens (Dunn) Nakai alleviates UVB-induced skin photoaging damage through the inhibition of MMP-1/3 and MAPK/AP-1 pathways in vitro and in vivo. *J. Funct. Foods* **2025**, *129*, 106890. [CrossRef]

Disclaimer/Publisher's Note: The statements, opinions and data contained in all publications are solely those of the individual author(s) and contributor(s) and not of MDPI and/or the editor(s). MDPI and/or the editor(s) disclaim responsibility for any injury to people or property resulting from any ideas, methods, instructions or products referred to in the content.